Fractal disperse hydrogen sorption kinetics in spark discharge generated Mg/NbO_x and Mg/Pd nanocomposites

Anca Anastasopol,[1,a)] Tobias V. Pfeiffer,[2] Andreas Schmidt-Ott,[2] Fokko M. Mulder,[1] and Stephan W. H. Eijt[1]
[1]*Department of Radiation, Radionuclides and Reactors, Delft University of Technology, Mekelweg 15, NL-2629 JB, Delft, The Netherlands*
[2]*Department of Chemical Engineering, Delft University of Technology, Julianalaan 136, NL-2628 BL, Delft, The Netherlands*

(Received 12 July 2011; accepted 15 October 2011; published online 8 November 2011)

Isothermal hydrogen desorption of spark discharge generated Mg/NbO_x and Mg/Pd metal hydride nanocomposites is consistently described by a kinetic model based on multiple reaction rates, in contrast to the Johnson-Mehl-Avrami-Kolmogorov [M. Avrami, J. Phys. Chem. **9**, 177 (1941); W. A. Johnson and R. F. Mehl, Trans. Am. Inst. Min., Metal. Eng. **135**, 416 (1939); A. N. Kolmogorov, Izv. Akad. Nauk SSSR, Ser. Mat. **3**, 355 (1937); F. Liu, F. Sommer, C. Bos, and E. J. Mittemeijer, Int. Mat. Rev. **52**, 193 (2007)] model which is commonly applied to explain the kinetics of metal hydride transformations. The broad range of reaction rates arises from the disperse character of the particle size and the dendritic morphology of the samples. The model is expected to be generally applicable for metal hydrides which show a significant variation in particle sizes, in configuration and/or chemical composition of local surroundings of the reacting nanoparticles. © *2011 American Institute of Physics*. [doi:10.1063/1.3659315]

In the context of hydrogen storage, MgH_2 remains an attractive candidate despite its relatively high stability and slow sorption kinetics. The latter can be substantially increased using small grain sizes[1] and adding transition metals or their oxides. In particular, niobium[2] and palladium[3,4] have a pronounced impact on the sorption kinetics. Previous studies[4–6] showed that spark discharge generation (SDG) is a versatile method for the production of metal nanoparticles. In particular, the onset of hydrogen desorption of spark discharge produced MgH_2 nanoparticles loaded from the gas phase occurs at a rather low temperature of ~400 K.[5] The hydrogen desorption is characterized by a broad desorption profile, which could be explained in terms of multiple apparent activation energies.

Here, we present a systematic study of the isothermal hydrogen desorption kinetics of spark discharge Mg/NbO_x and Mg/Pd nanocomposites loaded from the gas phase. We found that a kinetic model based on multiple reaction rates within the sample can consistently describe the results from our studies, in contrast to the Johnson-Mehl–Avrami-Kolmogorov (JMAK) model,[7–10] applied to metal hydride transformation kinetics, and explains the transformation as a homogeneous nucleation and growth process. The broad range of reaction rates arises from the disperse character of the particle size distribution and the dendritic morphology of the SDG samples.

A dual spark generator setup[5] was used for the production of Mg nanoparticles and for the intermixing with spark discharge generated Pd or Nb catalyst particles *in-situ* in the spark discharge reactor. The frequency of the 40 mJ Mg sparks is 300 Hz. In order to produce a targeted amount of a few at. % of catalyst, the second spark is operated with 14 mJ pulses at a frequency of 34 Hz. The samples were loaded in a hermetically closed sample holder in an Ar glovebox. Transmission electron microscopy (TEM) was performed on a FEI TECNAI TF20 monochromatic electron microscope at 200 kV. The x-ray diffraction (XRD) was performed using a Panalytical X'pert Pro PMD diffractometer with a Cu Kα source ($\lambda = 1.54187$ Å) with an X'Celerator line detector. The Rietveld refinement of the spectra was performed using the GSAS software package. The hydrogen desorption kinetics was measured in a home built temperature programmed desorption (TPD) setup.[5] Hydrogen loading before each desorption run was performed at 6.2 bar at 573 K for 6 h. Hydrogen unloading was performed at various temperatures for 20 h under vacuum of approximately 10^{-5} mbar. The rate of hydrogen desorbed was monitored using a quadrupole mass spectrometer.

A representative TEM image of the Mg/NbO_x nanocomposite sample presented in Fig. 1 indicates a uniform dispersion of Nb-containing particles intermixed with the Mg particles, as confirmed using energy-dispersive x-ray spectroscopy (EDS). The corresponding XRD pattern in Fig. 1 showed the presence of hexagonal Mg with crystallite sizes of ~30 nm, similar to the Mg/Pd sample. The crystalline

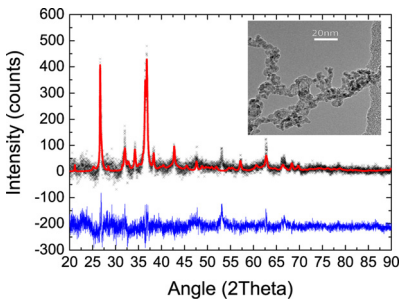

FIG. 1. (Color online) XRD pattern and Rietveld refinement of Mg/NbO_x nanocomposites produced by SDG (black are the data points, red the fit, and blue the residual). Inset shows a representative TEM image of the sample as-produced. Dark spots are Nb-containing particles.

a)Electronic mail: a.middelkoop-anastasopol@tudelft.nl.

Nb-compounds in the as-produced sample mainly consisted of Nb_2O_5 and NbO_2. TEM images of the Mg/Pd nanocomposites showed a similar dendritic morphology.[5]

The hydrogen desorption curves at 200 °C, 250 °C, and 300 °C for the Mg/Pd sample are depicted in Fig. 2. Similar curves are measured for the Mg/Nb sample (see our supporting information, Fig. S1).[11] The total amount of hydrogen desorbed is up to 1 wt. % depending on temperature. Clearly, the hydrogen desorption becomes systematically faster at higher temperatures. While the experimental desorption curves initially show a fast decay, they subsequently show a slower decaying tail relative to a simple exponential decay. The curves could be fitted satisfactorily by two exponential terms but only upon including an unrealistically high background term. We found that an adequate description involves the use of a stretched exponential decay, according to

$$I(t)/I_0 = a \cdot \exp(-(k_1 \cdot t)^n) + (1-a) \cdot \exp(-k_2 \cdot t), \quad (1)$$

with $I(t)/I_0$ the normalized hydrogen desorption rate, a the relative intensity of the stretched exponential, k_1 and k_2 reaction constants, and n the fractional exponent. The addition of a simple exponential term was necessary to fit the tail of the curve. In Fig. 3, the experimental desorption curves for the Mg/NbO_x sample are replotted according to $ln(-ln(I(t)/I_0))$ versus $ln(t)$, demonstrating the validity of this approach. A stretched exponential decay will result in a straight line in these plots with a slope equal to the value of the fractional exponent. Clearly, the kinetic curves in Fig. 3 closely follow a straight line, with an additional bending at the longest timescales, which could be properly accounted for by adding the simple exponential decay term describing the contributions of the slowest particles. A similar behavior was observed for the Mg/Pd sample (see our supporting information, Fig. S2).[11] The kinetic parameters obtained from the fits of the desorption curves are provided in our supporting information (Tables S1 and S2).[11]

Under specific conditions, when the phase nucleates randomly throughout the volume of the sample and grows at a constant growth rate, the JMAK model also predicts a stretched exponential decay for hydrogen sorption kinetics. For the case of three-dimensional growth, a fractional exponent $n \geq 3$ is obtained. This simple mechanism, nevertheless, does not fit most solid state reactions,[12] hence numerous special cases of the JMAK model for the growth mechanism of the nucleated phase were studied.[7] The fractional exponents found in this study, however, are systematically lower

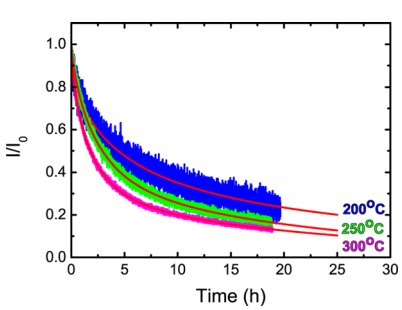

FIG. 2. (Color online) Isothermal hydrogen desorption of Mg/Pd nanocomposites at 200 °C, 250 °C, and 300 °C. Dotted lines represent best fits according to Eq. (1).

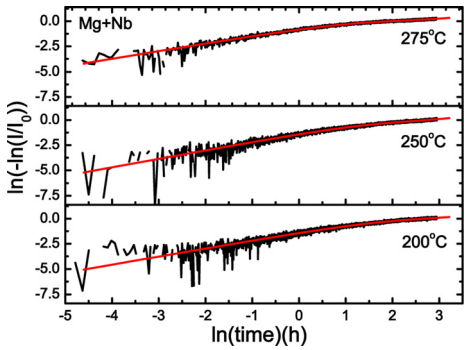

FIG. 3. (Color online) Double logarithmic analysis of the isothermal hydrogen desorption of Mg/NbO_x nanocomposites at 200 °C, 250 °C, and 275 °C. Solid lines are best fit results according to Eq. (1).

than 1, typically in the range of 0.55 to 0.85, for all fits, which cannot be explained in the currently available versions of the JMAK model.

We found that a kinetic model based on the presence of a wide range of reaction rates within the sample can consistently describe the results from our studies. Both spark discharge generated samples have a distribution of particle sizes and a complex dendritic morphology evident from TEM (Fig. 1), leading to strong local variations in the sample which violate the presumption of the same nucleation and growth conditions throughout the sample. Dispersion in the reactivity of solid state reactions has been applied to describe oxidation of organic or polymeric glasses[13,14] and free radical recombination reactions.[15] The origin of heterogeneity in the reaction rates within one sample can be either different configurations of the reacting particles or the varying chemical composition of the surroundings.[16,17]

Such a disperse solid sample can effectively be described as a sum of subsystems, each characterized by a different rate constant. If each subsystem reacts according to the first order kinetic law, then the rate of the transformation for the whole ensemble of subsystems is described by $I(t)/I_0 = \int_0^\infty H(k) \cdot \exp(-k \cdot t)dk$, where k is the rate constant, $H(k)$ is the distribution of rate constants and the inverse Laplace transform of $I(t)$, normalized according to $\int_0^\infty H(k)dk = 1$, and t is the desorption time.

A general analytical approximation for the shape of $H(k)$ was derived by Saito and Murayama,[18] according to

$$H(k) = \frac{bn}{(1-n)\sqrt{2\pi n}}(kb)^{\frac{-n+2}{2n-2}}\exp\left[-(kb)^{\frac{n}{n-1}}\right], \quad (2)$$

with $b = \left(k_1 n(1-n)^{(1-n)/n}\right)^{-1}$, where n is the fractional exponent, k is the reaction constant and k_1 is the reaction constant of the stretched exponential in Eq. (1). The rate constant distributions $H(k)$ calculated for the Mg/NbO_x and Mg/Pd samples are plotted in Fig. 4. In all cases, a broad distribution of rate constants is observed. The distributions of the Mg/NbO_x maintain nearly the same shape with increasing temperature (Fig. 4(a)), while they systematically shift towards higher k with increasing temperatures, reflecting faster sorption. The Mg/Pd sample presents a slightly different kinetic profile at 200 °C, when it reacts slowly compared to Mg/NbO_x, while a similar distribution is observed at 250 °C and 300 °C.

The temperature dependence of the rate constant distributions is better understood upon realizing that the rate

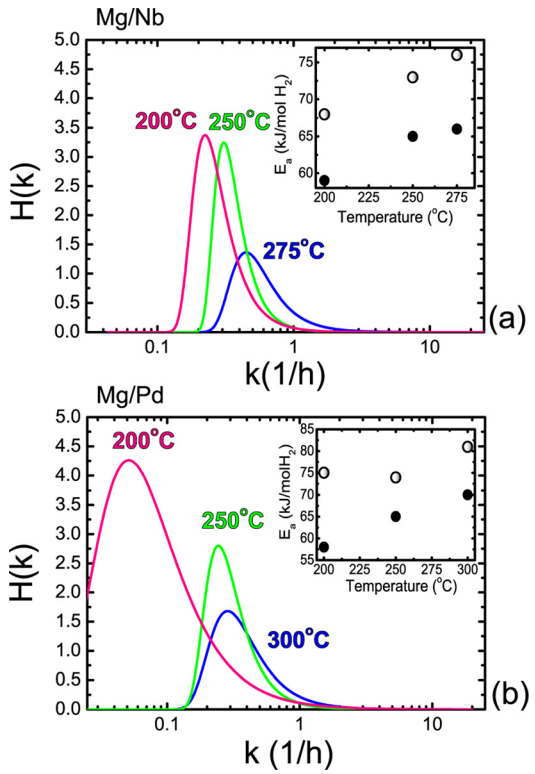

FIG. 4. (Color online) Hydrogen desorption reaction rate distributions $H(k)$ of (a) Mg/NbO_x; (b) Mg/Pd at various temperatures. The insets present the lower (filled circles) and higher (open circles) boundary of the activation energies derived from $H(k)$.

constants typically follow an Arrhenius behavior with temperature, according to $k = A\exp(-E_a/RT)$, where A is a preexponential factor, E_a is the apparent activation energy for the process,[19] R is the gas constant, and T is the temperature. Assuming that the preexponential factor A is a constant and equal to $1.2 \cdot 10^3 s^{-1}$ as obtained from Kissinger analysis in our previous desorption study,[5] values for the involved activation energies E_a can be derived. In the insets of Figs. 4(a) and 4(b), the activation energies corresponding to the lower and higher boundaries of the broad k distribution curves are plotted, defined by the respective k values at 1% of the maximum intensity of the distribution.

At 200 °C, the extracted lowest activation energy of ~58 kJ/mol is representative of the fastest reacting parts of the samples, i.e., the smallest sized particles,[5,20] as judged from a comparison with the broad overall distribution of apparent activation energies deduced in our previous study,[5] which starts at about 55 kJ/mol. The observed spread in contributing activation energies ranges from 8 kJ/mol to 17 kJ/mol. With increasing temperature, the slower reacting parts of the samples with apparent activation energies up to ~80 kJ/mol start to contribute to the hydrogen desorption. The contribution of simple exponential term with very low reaction rates of $k_2 \sim 0.015h^{-1} - 0.04h^{-1}$ reflects the slower reacting part of the sample. This is probably related to coverage of part of the MgH_2 nanoparticles with thin MgO shells of up to ~2 nm, leading to high apparent activation energies up to ~120 kJ/mol.[5] Part of the sample therefore does not desorb in the temperature range of 200–300 °C studied here, supported by our XRD study which revealed the presence of a small fraction of ~7 wt. % MgH_2 in the desorbed samples. Further prevention of partial oxidation during the synthesis process therefore may lead to fast desorption kinetics for spark discharge MgH_2 particles, for which apparent activation energies as low as 58 kJ/mol can be achieved.

Summarizing, we found that a distribution of reaction rates is a more appropriate description for the spark discharge generated MgH_2 nanoparticles, rather than the conventional homogeneous nucleation and growth mechanism of the JMAK model. This model for the hydrogen sorption kinetics is expected to be generally applicable for metal hydride nanoparticles with a clear particle size distribution, a complex (dendritic) morphology and/or coverage with oxides forming a barrier for hydrogen sorption. We note that a detailed knowledge of the size and shape distributions could aid to establish a quantitative link to the observed hydrogen desorption behavior.[21] Such size and shape dependence is an interesting topic of future research. The reaction rates distributions can be straightforwardly calculated from the stretched exponential decay of the hydrogen desorption. We deduced that at each temperature, only a part of the sample contributes to hydrogen desorption, corresponding to a temperature dependent specific window of apparent activation energies that characterize the active parts of the samples. Selection of the smallest particle sizes and further prevention of oxidation may lead to very low activation energies and fast hydrogen desorption at low temperatures.

This work was financially supported by NL Agency, Dutch Ministry of Economic Affairs, through the EOS grant LT07052.

[1]A. Zaluska, L. Zaluski, and J. O. Strom-Olsen, J. Alloys Compd. **288**, 217 (1999).
[2]H. G. Schimmel, J. Huot, L. C. Chapon, F. D. Tichelaar, and F. M. Mulder, J. Am. Chem. Soc. **127**, 14348 (2005).
[3]X. Xu and C. Song, Appl. Catal., A **300**, 130 (2006).
[4]V. A. Vons, H. Leegwater, W. J. Legerstee, S. W. H. Eijt, and A. Schmidt-Ott, Int. J. Hydrogen Energy **35**, 5479 (2010).
[5]V. A. Vons, A. Anastasopol, W. J. Legerstee, F. M. Mulder, S. W. H. Eijt, and A. Schmidt-Ott, Acta Mater. **59**, 3070 (2011).
[6]N. Tabrizi, M. Ullmann, V. Vons, U. Lafont, and A. Schmidt-Ott, J. Nanopart. Res. **11**, 315 (2009).
[7]F. Liu, F. Sommer, C. Bos, and E. J. Mittemeijer, Int. Mater. Rev. **52**, 193 (2007).
[8]M. Avrami, J. Phys. Chem. **9**, 177 (1941).
[9]W. A. Johnson and R. F. Mehl, Trans. Am. Inst. Min., Metall. Pet. Eng. **135**, 416 (1939).
[10]A. N. Kolmogorov, Izv. Akad. Nauk SSSR, Ser. Mat. **3**, 355 (1937).
[11]See supplementary material at http://dx.doi.org/10.1063/1.3659315 for the hydrogen desorption curves for the Mg/NbOx sample (Fig. S1), the $ln(-ln(I(t)/I_0))$ versus $ln(t)$ plots for the Mg/Pd sample (Fig. S2), and fit parameters obtained for the Mg/NbO_x and Mg/Pd samples (Table S1 and Table S2, respectively).
[12]J. Malek, Thermochim. Acta **267**, 61 (1995).
[13]I. Avramov, Thermochim. Acta **280–281**, 363 (1996).
[14]M. C. Weinberg, J. Non-Cryst. Solids **255**, 1 (1999).
[15]T. Doba, K. U. Ingold, and W. Siebrand, Chem. Phys. Lett. **103**, 339 (1984).
[16]E. Y. Davydov, A. P. Vorotnikov, and G. B. Pariyskii, *Kinetic Peculiarities of Solid Phase Reactions* (Wiley, London, 1998), pp. 5–24.
[17]V. A. Tolkatchev, Chem. Phys. **116**, 283 (1987).
[18]R. Saito and K. Murayama, Solid State Commun. **63**, 625 (1987).
[19]The apparent activation energy includes the energy of formation of hydrogen vacancies and interstitials and kinetic factors such as the migration energy of the interstitial and/or of the surface energy barrier for formation of hydrogen molecules.
[20]W. Li, C. Li, H. Ma, and J. Chen, J. Am. Chem. Soc. **129**, 6710 (2007).
[21]M. H. Mintz and Y. Zeiri, J. Alloys Compd. **216**, 159 (1994).